

Rotation, magnetism, and metallicity of M dwarf systems [★]

D. Shulyak^{1†}, A. Seifahrt^{1,2}, A. Reiners¹, O. Kochukhov³, N. Piskunov³

¹*Institute of Astrophysics, Georg-August-University, Friedrich-Hund-Platz 1, D-37077 Göttingen, Germany*

²*Department of Physics, University of California, One Shields Avenue, Davis, CA 95616, USA*

³*Department of Physics and Astronomy, Uppsala University, Box 516, 751 20, Uppsala, Sweden*

5 November 2018

ABSTRACT

Close M-dwarf binaries and higher multiples allow the investigation of rotational evolution and mean magnetic flux unbiased from scatter in inclination angle and age since the orientation of the spin axis of the components is most likely parallel and the individual systems are coeval. Systems composed of an early (M0.0 – M4.0) and a late (M4.0 – M8.0) type component offer the possibility to study differences in rotation and magnetism between partially and fully convective stars. We have selected 10 of the closest dM systems to determine the rotation velocities and the mean magnetic field strengths based on spectroscopic analysis of FeH lines of Wing-Ford transitions at 1 μm observed with VLT/CRIRES. We also studied the quality of our spectroscopic model regarding atmospheric parameters including metallicity. A modified version of the Molecular Zeeman Library (MZL) was used to compute Landé g-factors for FeH lines. Magnetic spectral synthesis was performed with the SYNMAST code. We confirmed previously reported findings that less massive M-dwarfs are braked less effectively than objects of earlier types. Strong surface magnetic fields were detected in primaries of four systems (GJ 852, GJ 234, LP 717-36, GJ 3322), and in the secondary of the triple system GJ 852. We also confirm strong 2 kG magnetic field in the primary of the triple system GJ 2005. No fields could be accurately determined in rapidly rotating stars with $v \sin i > 10$ km/s. For slow and moderately rotating stars we find the surface magnetic field strength to increase with the rotational velocity $v \sin i$ which is consistent with other results from studying field stars.

Key words: stars: atmospheres – stars: low-mass – stars: binaries: spectroscopic – stars: rotation – stars: magnetic fields.

1 INTRODUCTION

Stellar rotation plays an important role in the evolution of single and multiple systems, influencing the internal structures of stars, mixing processes, surface temperature-pressure structure, convection, and, of course, generation of the magnetic fields in subphotospheric layers where strong differential rotation takes place. In case of Sun-like and low-mass stars, rotational velocity was found to decrease with time (Skumanich 1972; Barnes 2007). Furthermore, this evolution of rotation seems to work differently for dM stars with fully convective envelopes. These objects are apparently not braked that much, and field dwarfs of spectral type late-M or L were found to rotate more rapidly than their higher mass siblings (Mohanty & Basri 2003; Reiners & Basri 2008).

The loss of angular momentum is caused by the stellar

wind which is driven by shock waves generated in atmospheres of solar type and cooler stars where the surface convection is strong enough to induce ultrasonic motions. On the other hand, the efficiency of mass loss probably depends on the intensity and geometry of the surface magnetic field (Mestel 1984; Kawaler 1988; Sills et al. 2000). These fundamental characteristics of the magnetic field are determined by the mechanism of its generation. Around spectral type M3.5, stars are believed to become fully convective and thus the dynamo mechanism must be different in cooler objects because they do not possess a tachocline layer with strong differential rotation. Therefore, if the magnetic field geometry changes in fully convective stars, a change in the braking law may appear as well. An observed lack of slowly rotating objects of spectral type later than mid-M could be a consequence of such a change in the net braking. A problem in the interpretation of stellar observations is that “in general” ages and other parameters like the angle of inclination (important in observations of $v \sin i$) are unknown, at least in field stars.

[★] Based on observations made with ESO Telescopes at the Paranal Observatories under programme ID 81.D-0189

[†] E-mail: denis.shulyak@gmail.com

Close double and hierarchical multiple system, however, are ideal probes to study the rotational evolution of late-M objects. Their components are most likely coeval and their spin axis aligned. Disc orientations in pre-main sequence stars (Monin et al. 2006) and orbit orientations in multiple systems (Sterzik & Tokovinin 2002) are partially correlated, and Bate et al. (2000) find that strong misalignments are unlikely in binaries with separations ≤ 100 AU. Thus, we may assume that the inclination angles i of close binary and multiple systems are near parallel. This allows direct insight in spectral type dependent rotational braking and its connection to magnetic field strength.

A first study of this kind was recently published by Reiners et al. (2007) based on the analysis of the close system LHS 1070 (GJ 2005) composed of a mid-M star (M5.5) and two fainter components B and C with spectral types around M9.0. Measuring the astrometric orbit of B and C , Leinert et al. (2000) determined masses at the limit to brown dwarfs. The full orbital solution of the system shows both orbits of this triple system to be co-planar within 2 degrees (Seifahrt et al. 2008), confirming the orbital alignment. It was found that magnetic flux in the B component is about twice as strong as in component C at similar rotation rate. Reiners et al. (2007) concluded that rotational braking is probably not proportional to magnetic field strength in fully convective objects, and that a different field topology could be the reason for the observed weak braking.

Motivated by the work of Reiners et al. (2007), we present an analysis of seven carefully selected binary systems and two multiple systems. Since the all components of multiple systems are results of the same star formation process with presumably identical age and metallicity, this allows us to study an evolution of the rotational velocities from a well defined sample of stars. Using high-resolution VLT/CRIRES observations of FeH lines at $\lambda\lambda 9920 - 9970$ we attempt to measure rotational velocities $v \sin i$ and mean surface magnetic field (B_s) in primary and secondary components and to search for the links between rotational braking, spectral type, and intensity of the surface magnetic field.

2 OBSERVATIONS

The data were obtained in service mode between July and September 2008 with the NIR spectrograph CRIRES mounted at UT1 of the VLT (programme ID 81.D-0189). Observations followed a simple ABBA on-slit nod scheme, collecting 4–10 spectra with individual exposure times of 180–300s, depending on the brightness of the individual targets. For all observations, both binary components were carefully aligned in the entrance slit and nod throws were chosen to avoid overlaps of both sources between A and B beams.

Data reduction followed the standard scheme of non-linearity correction of all raw frames, pairwise subtraction of the science frames to remove the sky background and flatfielding. 1D spectra were extracted from the individual flatfielded and sky subtracted frames using an optimum extraction algorithm and by carefully masking the nearby component to exclude flux contamination in those close double stars. Due to the inherent slit curvature of CRIRES, spectra taken in different nodding positions do not share the same

wavelength scale. To correct for this effect we calculated individual wavelength solutions. We then mapped all 1D spectra onto a common wavelength grid and finally co-added all rebinned spectra of each component. The wavelength solutions are based at first order on the ThAr calibration frames provided by ESO and were refined by matching the science spectra to the atlas of GJ1002, previously observed with CRIRES (Wende et al. 2010).

Table 1 summarises some information about the observed systems, including the observed separation of the components in our CRIRES spectra as well as the distance to the system which is mostly based on trigonometric parallaxes. In addition, we indicate which systems are identified in the literature as being younger than 300 Myrs, based on their membership in a young moving group or by showing low surface gravity and strong X-ray and H α activity.

We also extended the original sample of stars by GJ 2005, a triple system analysed previously by Reiners et al. (2007). This system was also observed with CRIRES (programme ID 60.A-9078). Unfortunately, the components of the system GJ 3344 (LHS 1749) could not be spatially disentangled due to strong orbital motion between the discovery of this binary and our observations. We could thus not perform individual analysis of each of the components and excluded the system from our investigation. For all other systems, we obtained individual spectra of components, though the signal-to-noise ratio is very low for some of them (mostly for the fainter B and C components).

3 METHODS

3.1 Input line lists and synthetic spectra

In our investigation we employed the FeH line list of the Wing-Ford band ($F^4 \Delta - X^4 \Delta$ transitions at $1 \mu\text{m}$) and molecular constants taken from Dulick et al. (2003)¹. For some of these lines we used corrected Einstein A values according to Wende et al. (2010).

To compute synthetic spectra of the atomic and molecular lines in the presence of a magnetic field, we employed the SYNMAST code (Kochukhov 2007). The code represents an improved version of the SYNTHMAG code described by Piskunov (1999). It solves the polarized radiative transfer equation for a given model atmosphere, atomic and molecular line lists and magnetic field parameters. The code treats simultaneously thousands of blended absorption lines, taking into account their individual magnetic splitting patterns, which can be computed for the Zeeman or the Paschen-Back regime. SYNMAST provides local four Stokes parameter spectra for a number of angles between the surface normal and the line of sight (7 by default). These local spectra are convolved with appropriate rotational, macroturbulent and instrumental profiles and then combined to simulate the stellar flux profiles.

Model atmospheres are from the recent MARCS grid² (Gustafsson et al. 2008).

¹ <http://bernath.uwaterloo.ca/FeH/>

² <http://marcs.astro.uu.se>

Table 1. M-dwarf systems.

Name	Spectral type	SNR	Separation, $\rho \pm 0.1$, arcsec	Distance, pc	Age (Young?)	Reference
GJ 852	<i>A</i> M4.0	260	7.8 (<i>A-C</i>) 0.9 (<i>B-C</i>)	10.0	no	1, 3
	<i>B</i> M4.5	170				
	<i>C</i> M7.0 ^a	40				
GJ 4368 (LHS 4022)	<i>A</i> M4.0	300	1.3	11.0	no	1, 4
	<i>B</i> M5.5	140				
LTT 7419	<i>A</i> M2.5	250	15.5	10.0 ^b	no	5
	<i>B</i> M7.0 ^a	20				
GJ 234	<i>A</i> M4.5	100	1.0	4.1	no	6, 7
	<i>B</i> M7.0	100				
LP 717-36	<i>A</i> M3.5	120	0.5	20.2	yes	2, 3, 8, 9
	<i>B</i> M4.0	100				
GJ 3322 (LP 476-207)	<i>A</i> M4.0	170	1.2	32.1	yes	10, 11, 12
	<i>B</i> M5.0 ^a	90				
GJ 3304	<i>A</i> M4.0	70	0.8	14.5	yes	1, 4, 8, 9
	<i>B</i> M4.5	50				
GJ 3263 (LHS 1630)	<i>A</i> M3.5	120	0.9	13.3	no	1, 4
	<i>B</i> M4.0 ^a	80				
GJ 3344 ^c (LHS 1749)	<i>A</i> M2.0	110	~	~	~	~
	<i>B</i> M5.0					
GJ 2005 (LHS 1070)	<i>A</i> M5.5	50	1.35 (<i>A-B</i>) 1.75 (<i>A-C</i>)	7.7	no	13, 14, 15
	<i>B</i> M8.5	20				
	<i>C</i> M9.0	20				

^a No spectral type was available in the literature. Spectral types are determined based on the spectral type of the primary and the near-infrared magnitude difference of the components.

^b No distance measurement available in the literature. Spectro-photometric distance estimate is based on the V-K color of the primary which agrees with the distance obtained from the R-K color of the secondary, assuming a spectral type of M7.

^c Double-lined binary, components could not be spatially disentangled.

References for spectral types, distances, and youth:

1 - Beuzit et al. (2004), 2 - Reid et al. (2004), 3 - Riaz et al. (2006), 4 - Hawley et al. (1997), 5 - Jao et al. (2003), 6 - Kirkpatrick et al. (1991), 7 - Buscombe & Foster (1995), 8 - Daemgen et al. (2007), 9 - Shkolnik et al. (2009), 10 - Delfosse et al. (1999), 11 - Song et al. (2003), 12 - Lépine et al. (2009), 13 - Leinert et al. (2000), 14 - Costa et al. (2005), 15 - Reiners et al. (2007).

3.2 Molecular Zeeman effect

In order to analyse the magnetic field through spectral synthesis it is necessary to know the Landé *g*-factors of upper and lower levels of a particular molecular transition. As to diatomic molecules, a simple analytical expression for *g*-factors can be obtained only in special cases of pure Hund's *A* and *B* splitting of energy levels. These cases correspond to the strong and weak coupling of the electronic spin **S** and orbital **L** momenta to the internuclear axis (i.e. coupling with nuclear rotation) (see Herzberg 1950). Unfortunately, as stated in Berdyugina & Solanki (2002), the lines of FeH of the Wing-Ford band exhibit splitting that is in most cases intermediate between pure Hund's *A* and *B* and which is not trivial to treat both theoretically and numerically. Available theoretical descriptions make use of the approach based on the so-called effective Hamiltonian that is usually represented as a sum of the unperturbed part describing energies of Zeeman levels as they undergo transition between Hund's cases, and the part describing an interactions with the external magnetic field. A detailed description can be found, for example, in Berdyugina & Solanki (2002) and Asensio Ramos & Trujillo Bueno (2006).

To compute *g*-factors we implement numerical libraries from the MZL (Molecular Zeeman Library) package orig-

inally written by B. Leroy (Leroy 2004), and adopted for the particular case of FeH. MZL is a collection of routines for computing the Zeeman effect in diatomic molecules, and it contains all the physics of pure and intermediate Hund's cases presented in Berdyugina & Solanki (2002). Due to the limitations of the theoretical description of the intermediate Hund's case presented in Berdyugina & Solanki (2002), the calculated *g*-factors in most cases fail to fit the observed splitting of FeH lines. This has already been mentioned in a number of previous investigations (see Afram et al. 2008; Berdyugina & Solanki 2002; Harrison & Brown 2008). Therefore, in the present investigation we used an alternative approach described in Shulyak et al. (2010). The authors suggested a semi-empirical method of computing *g*-factors using MZL routines and different Hund's cases for upper and lower energy levels of particular FeH transitions depending on their quantum numbers and the fit to the spectra of a sunspot with known magnetic field intensity. This approach has been successfully applied to the analysis of the magnetic field in FeH spectra of several magnetic M-dwarfs and we refer the interested reader to the original work by Shulyak et al. (2010).

3.3 Analysis of the spectra

The spectroscopic estimation of the atmospheric parameters for each system is a complicated task because of the short wavelength region $\lambda\lambda 9920 - 9972$ observed with CRIRES. In spite of the fact that, in general, lines of FeH are good indicators of the atmospheric temperature and the magnetic field strength, no lines of other species (especially atoms) are present in this spectral range that could be used for cross-checking. Moreover, the van der Waals damping constants γ_{Waals} are unknown for FeH transitions. In case of slow rotation, pressure broadening is the dominating broadening mechanism in the dense plasma of dM stars, and thus the knowledge of γ_{Waals} is of high importance when it turns to quantitative analysis of individual line profiles. As found by Shulyak et al. (2010) and Wende et al. (2010), the classical γ_{Waals} (Gray 1992) must be increased by a factor of ≈ 3.5 to fit FeH lines in the spectra of non-magnetic M5.5 dwarf GJ 1002. Note that any uncertainties in γ_{Waals} would immediately affect the estimation of other parameters, such as $v \sin i$, Fe abundance $\alpha(\text{Fe})$, and T_{eff} . Hence, when analysing spectra of M-dwarfs, some of these key parameters must be known independently and prior to spectroscopic fitting. However, there is a strong evidence that γ_{Waals} drops significantly for late M's, and its value must be estimated using spectra of some non-magnetic stars. Here we made use of spectra of the weakly magnetic M8.0 star VB 10, but its rather high $v \sin i = 6$ km/s (Reiners & Basri 2007) makes it still difficult to precisely determine the FeH damping constant. Also, the analysis of Keck/HIRES spectra of three M8V dwarfs from a program of Reiners & Basri (2010) did not warrant accurate results, mainly because of low resolution of the data (see Sect. 4.1 for details). We therefore investigated for every system a possible range of atmospheric parameters under different assumptions about γ_{Waals} : since any uncertainties in T_{eff} or γ_{Waals} immediately transform into uncertainties of $v \sin i$ and $\alpha(\text{Fe})$ (and vice versa), it is essential to fix either T_{eff} or $\alpha(\text{Fe})$ and then search for the combination of remaining parameters (γ_{Waals} and $v \sin i$) that provides the best fit. Usually, spectral types are known from photometric calibrations. Here we utilise the effective temperature scale given in Kenyon & Hartmann (1995) for stars in the spectral type range [M0.0:M6.0] and from Golimowski et al. (2004) for [M6.5:M9.5] respectively. The reference abundance of iron is assumed to be solar $\alpha(\text{Fe}) = -4.59$ (Asplund et al. 2005). We also assume $\log(g) = 5.0$ for all objects in our sample which is the usual value for dM stars (Ségransan et al. 2003; Bean et al. 2006; Berger et al. 2006).

Finally, the basic steps of spectroscopic analysis can be summarized as follows:

(i) Using a set of magnetically insensitive FeH lines we derive fitting parameters such as $\alpha(\text{Fe})$, $v \sin i$, $f(\gamma_{\text{Waals}})$ (enhancement factor by which the classical γ_{Waals} is multiplied), and T_{eff} by least-square minimisation fit. The magnetic insensitive lines used are: FeH $\lambda\lambda 9941.62$, 9944.56 , 9945.83 , 9953.07 , 9957.30 , 9962.83 .

(ii) The intensity of the surface magnetic field $\langle B_s \rangle$ was determined by constructing a χ^2 goodness-of-the-fit landscape of the deviation between observed and predicted FeH spectra for a number of values of the magnetic field intensity.

(iii) In case of very fast rotating stars all the available

spectral range of $\lambda\lambda 9920 - 9972$ was fitted because of strong line blending. No accurate estimate of the magnetic field was possible for such objects.

To provide a comprehensive look into the possible parameter space of each stellar component, the following compilations of fitted parameters were considered:

- (i) determining $v \sin i$ with fixed T_{eff} , $\alpha(\text{Fe})$, and $f(\gamma_{\text{Waals}})$;
- (ii) determining T_{eff} and $v \sin i$ with fixed $\alpha(\text{Fe})$ and $f(\gamma_{\text{Waals}})$;
- (iii) determining $f(\gamma_{\text{Waals}})$ and $v \sin i$ with fixed T_{eff} and $\alpha(\text{Fe})$.

Using this approach we find rotational velocities and surface magnetic field intensities (where possible) using the SYNMAST code and Landé g-factors calculated as described in Shulyak et al. (2010). In the next section we present detailed results of our investigation.

4 RESULTS

4.1 Pressure broadening of FeH lines

Based on investigations of FeH lines in spectra of the non-magnetic and slowly rotating M5.5 dwarf GJ 1002 it was shown that to get a satisfactory agreement between observed and predicted spectra one needs a 3.5 times increase of the classical van der Waals damping constant γ_{Waals} (see Shulyak et al. 2010; Wende et al. 2010). To verify the behaviour of γ_{Waals} in much cooler plasma we analysed spectra of late type non- or weakly active M-dwarfs 2MASS-1246517+314811 (M7.5, $T_{\text{eff}} = 2550$ K), 2MASS-1440229+133923 (M8.0, $T_{\text{eff}} = 2500$ K), 2MASS-2037071-113756 (M8.0, $T_{\text{eff}} = 2500$ K) from Reiners & Basri (2010), and VB 10 (M8.0, $T_{\text{eff}} = 2500$ K). Assuming effective temperatures to be known from stellar spectral types and solar iron abundance, the fit to the observed spectra in all late M's resulted in a strong decrease of γ_{Waals} . For instance, for 2MASS-2037 an optimal fit is obtained with $f(\gamma_{\text{Waals}}) \approx 0.16$ and $v \sin i = 4$ km/s. Decreasing $v \sin i$ to 1 km/s results in only in marginal increase of $f(\gamma_{\text{Waals}})$. Even smaller $f(\gamma_{\text{Waals}}) \approx 0.06$ is found for 2MASS-1440 and 2MASS-1246. Thus, there is an unexpected difference in γ_{Waals} for these three stars as it should be (naively) lower for 2MASS-2037 than for the hotter 2MASS-1246, or at least nearly the same. We speculate that the explanation can be connected with a) a slightly different iron abundance in the atmospheres of these objects, b) uncertainties in spectral type determination, and/or c) the quality of the spectra (SNR).

The same conclusion follows from the analysis of the spectra of VB 10, which has the highest resolution of $R \approx 85000$ among the four targets, but, on the other hand, higher rotational velocity. Assuming fixed $v \sin i = 6$ km/s from Reiners & Basri (2007) results in $f(\gamma_{\text{Waals}}) = 0.3 \pm 0.01$, i.e. even larger than the value found for 2MASS-2037. Fixing $f(\gamma_{\text{Waals}}) = 3.5$ needs a substantial decrease of $v \sin i = 1.18$ km/s and $\alpha(\text{Fe}) = -5.28$, however with slightly better fit. Increasing T_{eff} from 2500 K to 2600 K and fixing solar $\alpha(\text{Fe}) = -4.59$ and $v \sin i = 6$ km/s gives again better fit but larger $f(\gamma_{\text{Waals}}) \approx 0.74$ and $\gamma_{\text{Waals}} \approx 2$ for even higher

$T_{\text{eff}} = 2700$ K, respectively. Note that the error bars for spectral type of M-dwarfs are usually ± 0.5 which translates to a minimum error in temperature of approximately ± 50 K. Therefore, $T_{\text{eff}} = 2700$ K for VB 10 seems not well justified, and thus γ_{Waals} is likely to have values < 1.0 for late-type objects, but its true value is difficult to determine at the present stage. As an example, Fig. 1 illustrates theoretical fits to some of FeH lines.

As mentioned above, we assumed the same $\log(g) = 5.0$ for all early and late type dM stars. The later ones, however, may have larger $\log(g)$ values (see, e.g., Ségransan et al. 2003; Bean et al. 2006; Berger et al. 2006) that can reach up to 5.4 dex at spectral type M8.0. Obviously, this cannot help to resolve the issue with decrease in $f(\gamma_{\text{Waals}})$ for the coolest M dwarfs simply because higher $\log(g)$ would broaden profiles of spectral lines, thus requiring even smaller $f(\gamma_{\text{Waals}})$ than those found here.

Taking into account a certain difficulty to accurately estimate the pressure broadening constant, we thus examine for each binary system a set of solutions depending on assumed value of $f(\gamma_{\text{Waals}}) = [0.3, 1.0, 3.5]$. This allowed us to estimate a possible impact of the uncertainty in T_{eff} , $f(\gamma_{\text{Waals}})$, and $\alpha(\text{Fe})$ on final results (e.g., $v \sin i$ and $\langle B_s \rangle$). Note that in case of early type M stars we use mainly $f(\gamma_{\text{Waals}}) = [1.0, 3.5]$.

4.2 Atmospheric parameters of stars in dM systems

In this paragraph we present estimates of the $v \sin i$ and $\langle B_s \rangle$ obtained for three basic sets of fitted parameters introduced in Sect. 3.3.

Case 1: determining $v \sin i$ and $\langle B_s \rangle$ with fixed T_{eff} , $\alpha(\text{Fe})$, and $f(\gamma_{\text{Waals}})$

Formally, the easiest and the straightforward way of the analysis would be to assume that T_{eff} is known from the spectral type assigned to each star. Then, the iron abundance would be solar or nearly solar as all objects belong to solar neighborhood and their atmospheres are well mixed due to strong convection. The only issue left is the $f(\gamma_{\text{Waals}})$, which value is most uncertain. Nevertheless, it can be taken from recent investigations (Shulyak et al. 2010; Wende et al. 2010) for early-type objects and from the analysis given in Sect. 4.1 of this work for late-type ones. Theoretical computations showed, however, that fixing T_{eff} , $\alpha(\text{Fe})$, and $f(\gamma_{\text{Waals}})$ always resulted in the worst fit for all objects. Furthermore, setting $f(\gamma_{\text{Waals}}) = 1.0$ also did not improve the fit for both early- and late-type stars. This indicated that some of the fixed parameters must differ from assumed values, and in the next step we tried to explore how much could these differences be and what is their impact on estimated $v \sin i$ and $\langle B_s \rangle$.

Case 2: determining T_{eff} , $v \sin i$, and $\langle B_s \rangle$ with fixed $\alpha(\text{Fe})$ and $f(\gamma_{\text{Waals}})$

Keeping $\alpha(\text{Fe})$ fixed at its solar value and $f(\gamma_{\text{Waals}}) = [0.3, 3.5]$ for late- and early-type stars respectively allowed us to obtain a much better agreement between observed and

predicted profiles of FeH lines, and in many (but not all) cases this resulted in the best fit. Table 2 summarizes results for each system, and its inspection immediately leads to the following conclusion: in all cases the obtained T_{eff} deviates from the temperature estimated from the individual spectral type using calibrations after Kenyon & Hartmann (1995) and Golimowski et al. (2004). Large deviations are found for GJ 3304-A (283 K) and GJ 852-A (233 K). The deviation from the empirical T_{eff} -spectral type relation and the one derived here is plotted on the left panel of Fig. 2. Apart from the big scatter in the derived T_{eff} even for objects of the same spectral type, the run of T_{eff} roughly follows empirical predictions. We thus speculate that probably the spectral type was incorrectly assigned to some of our objects. Or, as will be shown below, the iron abundance of stars may differ from the solar one which we assumed here.

Case 3: determining $\alpha(\text{Fe})$, $v \sin i$, and $\langle B_s \rangle$ with fixed T_{eff} and $f(\gamma_{\text{Waals}})$

This combination of fitted parameters also provided a very good agreement between observed and predicted profiles of FeH lines and the results are presented in Table 3. In particular, keeping T_{eff} fixed immediately reflected in the strong changes of the iron abundance, which in some cases was found to be up to 0.5 dex lower or larger than its current solar value (e.g. GJ 4368-B, GJ 3304). Figure 3 shows derived iron abundance for each star. It is seen that for this case, $\alpha(\text{Fe})$ differs significantly among objects of the same system, which is difficult to understand from the physical point of view as naturally one would expect that all the components have the same abundance patterns due to their common origin and history. It is interesting that in most cases $\alpha(\text{Fe})$ of the primary is higher than that of the secondary. This may be a hint for an effect of the degeneracy between temperature and Fe abundance in our models. Consistent results are found for LP 7419 and GJ 3263. Values close to solar are found for GJ 852-B, LP 717-36-A, GJ 3322-A, and GJ 2005-BC.

The most interesting outcome of fixing T_{eff} and $f(\gamma_{\text{Waals}})$, however, is that the derived $v \sin i$ and $\langle B_s \rangle$ does not change much, and their values in Table 2 and Table 3 are in good agreement between each other. This is an important result since it tells us that even if our estimates of abundances and/or temperatures are wrong by any means, this has little influence on the derived rotational velocity and surface magnetic field. In case of rotation, fixing T_{eff} at a certain value simply requires the adjustment of $\alpha(\text{Fe})$ in order to obtain minimum deviation between observed and theoretical spectra. Note that fitting is done using magnetically insensitive FeH lines for slow and moderately rotating stars and thus this in no way influences estimates of the magnetic field. The estimated strength of the later is driven by Zeeman-broadened lines and thus should weakly depend on assumed T_{eff} and $\alpha(\text{Fe})$, of course if rotation is relatively slow. This is exactly what is seen from Table 3.

Case 4: determining T_{eff} , $v \sin i$, and $\langle B_s \rangle$ with fixed $f(\gamma_{\text{Waals}})$ and mean $\alpha(\text{Fe})$

As a last step in our spectroscopic analysis we determined T_{eff} and $v \sin i$, but this time assuming iron abundance to be

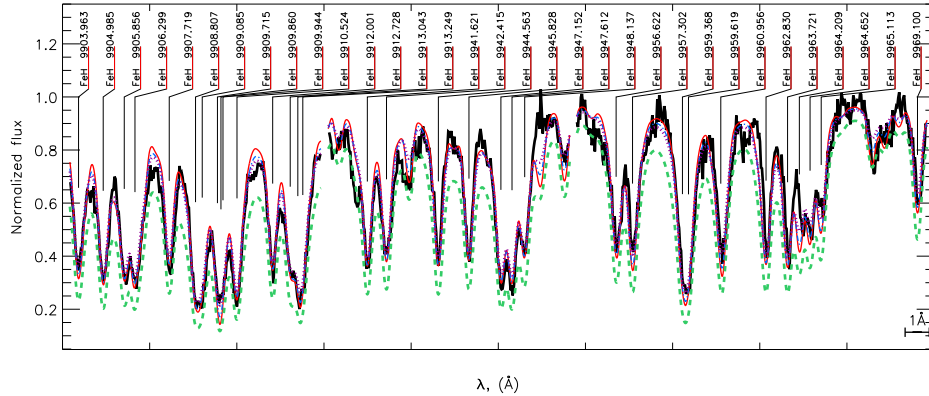


Figure 1. Comparison between observed and predicted profiles of FeH lines in spectra of M8.0 dwarf VB 10. Thick line – observations; thin full line (red) – $T_{\text{eff}} = 2500$ K, $f(\gamma_{\text{Waals}}) = 0.3$; dashed line (green) – $T_{\text{eff}} = 2500$ K, $f(\gamma_{\text{Waals}}) = 1.0$; dash-dotted line (blue) – $T_{\text{eff}} = 2600$ K, $f(\gamma_{\text{Waals}}) = 0.8$, dotted line (violet) – $T_{\text{eff}} = 2700$ K, $f(\gamma_{\text{Waals}}) = 2.0$. For all models solar Fe abundance and $v \sin i = 6$ km/s were used.

Table 2. Atmospheric parameters of M-dwarf systems, obtained under the assumption of fixed $\alpha(\text{Fe})$ and $f(\gamma_{\text{Waals}})$ (Case 2).

System	Component	Spectral type	$T_{\text{eff}}^{(0)}$ (K)	T_{eff} (K)	$\alpha(\text{Fe})$	$v \sin i$ (km/s)	$f(\gamma_{\text{Waals}})$	$ \mathbf{B} $ (kG)	χ^2 (GOF)
GJ 852	A	M4.0	3366	3133	-4.59	5.14	3.5	3	0.2836
	B	M4.5	3310	3132	-4.59	3.66	3.5	1.6	0.1644
	C	M7.0	2621	2582	-4.59	11.38	0.3	~	2.1322
GJ 4368 (LHS 4022)	A	M4.0	3366	3554	-4.59	3.01	3.5	0.5	0.0662
	B	M5.5	3250	3375	-4.59	2.80	3.5	0.79	0.1206
LTT 7419	A	M2.0	3525	3741	-4.59	3.62	3.5	0	0.0551
	B	M8.0	2621	2681	-4.59	12.35	0.3	~	2.8455
GJ 234	A	M4.5	3310	3152	-4.59	6.15	3.5	2.75	0.1731
	B	M7.0	2621	2737	-4.59	12.93	0.3	~	0.8577
LP 717-36	A	M3.5	3418	3346	-4.59	3.94	3.5	1.75	0.1123
	B	M4.0	3366	3163	-4.59	12.16	3.5	~	0.6185
GJ 3322 (LP 476-207)	A	M4.0	3366	3289	-4.59	6.75	3.5	3	0.1200
	B	M5.0	3250	3101	-4.59	23.77	3.5	~	0.4277
GJ 3304	A	M4.0	3366	3083	-4.59	29.73	3.5	~	0.3142
	B	M4.5	3310	3084	-4.59	45.35	3.5	~	0.2956
GJ 3263 (LHS 1630)	A	M3.5	3418	3600	-4.59	2.27	3.5	0.75	0.0930
	B	M4.0	3366	3518	-4.59	2.73	3.5	0.5	0.1178
GJ 2005 (LHS 1070)	A	M5.5	3160	2982	-4.59	6.82	3.5	2	0.1541
	B	M8.5	2450	<2500	-4.59	15.83	0.3	~	5.5399
	C	M9.0	2400	<2500	-4.59	15.06	0.3	~	5.9756

$T_{\text{eff}}^{(0)}$ is the temperature which corresponds to the spectral type of the star.

No accurate estimates of magnetic field were possible for stars with $v \sin i > 10$ km/s (marked with “~”)

Last column refer to the chi-square goodness of the fit (GOF) values.

For GJ 2005 only upper limit of T_{eff} can be derived because of temperature limitation of the available MARCS model grid.

identical for members of the same system and its values were simply taken as a mean of individual values from the Case 3 (see Table 3). Table 4 summarizes the obtained parameters. Again, and similar to previous case, neither rotational velocities nor the surface magnetic field changed much. Using a mean iron abundance, however, led to somewhat better agreement between derived and empirically calibrated effective temperatures, as can be seen from the right panel of Fig. 2. In particular, temperatures of objects of types M3.5 and M5.0 get closer to empirical values. Yet there still exist noticeable deviations between predicted and empirical values.

5 DISCUSSION

In our investigation we attempted to derive atmospheric parameters of seven spectroscopically resolved M-dwarf binary systems and two triple systems. Using advanced software for the calculation of molecular line formation in magnetized plasma and high-resolution CRIRES spectra allowed us to carry out accurate spectroscopic analysis. However, two main complications exist: 1) the narrow wavelength range of $\lambda\lambda 9920 - 9970$ observed with CRIRES does not allow an independent derivation of partially degenerate parameters as T_{eff} and $\alpha(\text{Fe})$. We could always find more than one solution. 2) Unknown van der Waals damping constants of FeH add another uncertainty to our measurements, es-

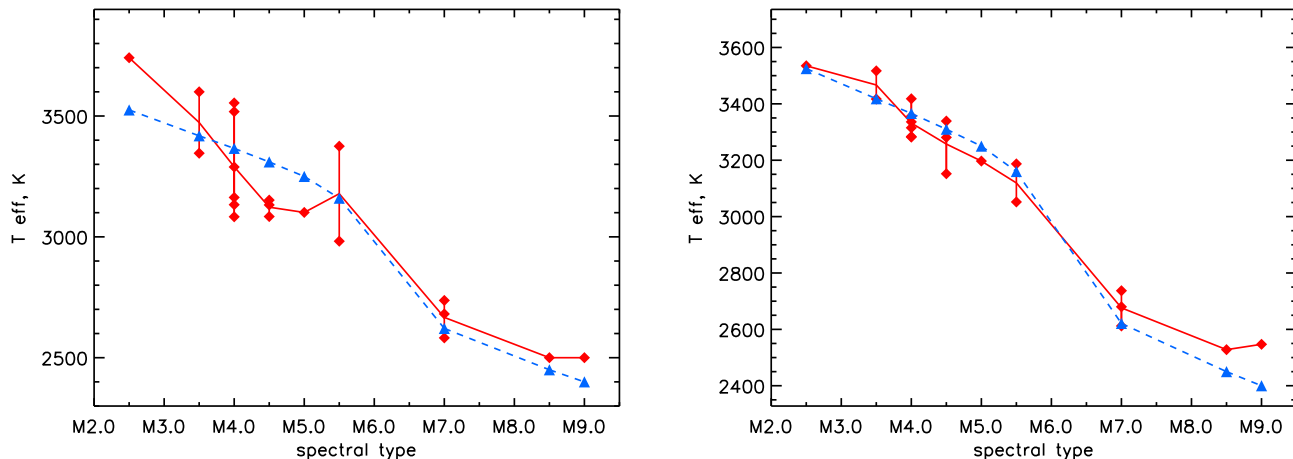


Figure 2. Run of the effective temperature as a function of spectral type derived from the FeH lines for Case 2 (**left panel**) and Case 4 (**right panel**). See text for more details. Red diamonds represent measurements for each individual object and solid line connects their mean values. Blue dashed line correspond to empirical calibrations after Kenyon & Hartmann (1995) and Golimowski et al. (2004).

Table 3. Atmospheric parameters M-dwarf systems, obtained under the assumption of fixed T_{eff} and $f(\gamma_{\text{Waals}})$ (Case 3).

System	Component	Spectral type	T_{eff} (K)	$\alpha(\text{Fe})$	$v \sin i$ (km/s)	$f(\gamma_{\text{Waals}})$	$ \mathbf{B} $ (kG)	χ^2 (GOF)
GJ 852	A	M4.0	3366	-4.16	5.43	3.5	3	0.4461
	B	M4.5	3310	-4.26	3.90	3.5	1.5	0.1749
	C	M7.0	2621	-4.48	11.35	0.3	~	2.2511
GJ 4368 (LHS 4022)	A	M4.0	3366	-4.83	2.74	3.5	0.5	0.0660
	B	M5.5	3160	-4.94	2.41	3.5	0.75	0.1249
LTT 7419	A	M2.5	3525	-4.80	3.40	3.5	0	0.0523
	B	M7.0	2621	-4.77	12.49	0.3	~	2.8463
GJ 234	A	M4.5	3310	-4.29	6.35	3.5	2.5	0.2249
	B	M7.0	2621	-4.92	13.12	0.3	~	0.7689
LP 717-36	A	M3.5	3418	-4.50	3.98	3.5	1.75	0.1145
	B	M4.0	3366	-4.24	12.17	3.5	~	0.6142
GJ 3322 (LP 476-207)	A	M4.0	3366	-4.49	6.82	3.5	3	0.1356
	B	M5.0	3250	-4.30	23.80	3.5	~	0.3949
GJ 3304	A	M4.0	3366	-4.05	29.19	3.5	~	0.2908
	B	M4.5	3310	-4.15	44.78	3.5	~	0.2642
GJ 3263 (LHS 1630)	A	M3.5	3418	-4.80	2.10	3.5	0.75	0.0922
	B	M4.0	3366	-4.79	2.52	3.5	0.5	0.1161
GJ 2005 (LHS 1070)	A	M5.5	3160	-4.18	6.89	3.5	1.75	0.1928
	B	M8.5	2500*	-4.52	15.94	0.3	~	5.7981
	C	M9.0	2500*	-4.58	15.11	0.3	~	5.9962

No accurate estimates of magnetic field were possible for stars with $v \sin i > 10$ km/s (marked with “~”)

Last column refer to the chi-square goodness of the fit (GOF) values.

(*) – coolest available model with $T_{\text{eff}} = 2500$ was used.

pecially for slow and moderately rotating stars where pressure broadening is one of the main line broadening agents. Thus, we attempted to search for a set of parameters (using chi-square technique) that provides a satisfactory fit to the data while still being within our expectations from a physical point of view. For example, effective temperature is expected to lie within a range predicted by the spectral type, and iron abundance should not be too different between components of the same systems and not too different from the solar one. However, this approach did not always lead to the best possible agreement between our model and the observed data. Varying T_{eff} turned out to be an effective

way to achieve better fit quality. In several systems the adopted T_{eff} differs from our expectations according to spectral types (for example, like M2.5 instead of M3.5 and M5.5 instead of M4.5 in case of LP 717-36-*A* and of GJ 234-*A* respectively), but differences are typically not larger than one spectral subclass. Such differences can easily be explained by varying Fe abundances. The distribution of the latter is usually within 0.3 dex for all systems except GJ 3304 if we assume the same Fe abundances for components of a given multiple system.

The possibility of achieving an acceptable fit quality under different assumptions and finally using quite different

Table 4. Atmospheric parameters M-dwarf systems, obtained under the assumption of fixed $\alpha(\text{Fe})$ and $f(\gamma_{\text{Waals}})$ (Case 4).

System	Component	Spectral type	$T_{\text{eff}}^{(0)}$ (K)	T_{eff} (K)	$\alpha(\text{Fe})$	$v \sin i$ (km/s)	$f(\gamma_{\text{Waals}})$	$ \mathbf{B} $ (kG)	χ^2 (GOF)
GJ 852	A	M4.0	3366	3282	-4.30	5.30	3.5	3	0.4011
	B	M4.5	3310	3281	-4.30	3.91	3.5	1.5	0.1706
	C	M7.0	2621	2680	-4.30	11.18	0.3	~	2.4740
GJ 4368 (LHS 4022)	A	M4.0	3366	3315	-4.89	2.71	3.5	0.5	0.0634
	B	M5.5	3160	3187	-4.89	2.49	3.5	0.75	0.1235
LTT 7419	A	M2.5	3525	3535	-4.79	3.41	3.5	0	0.0524
	B	M7.0	2621	2612	-4.79	12.68	0.3	~	2.8217
GJ 234	A	M4.5	3310	3152	-4.60	6.15	3.5	2.75	0.1731
	B	M7.0	2621	2737	-4.60	12.93	0.3	~	0.8577
LP 717-36	A	M3.5	3418	3517	-4.37	4.07	3.5	1.75	0.1172
	B	M4.0	3366	3284	-4.37	12.16	3.5	~	0.6119
GJ 3322 (LP 476-207)	A	M4.0	3366	3418	-4.40	6.94	3.5	2.75	0.1519
	B	M5.0	3250	3197	-4.40	23.80	3.5	~	0.4048
GJ 3304	A	M4.0	3366	3336	-4.10	29.26	3.5	~	0.2912
	B	M4.5	3310	3339	-4.10	44.51	3.5	~	0.2621
GJ 3263 (LHS 1630)	A	M3.5	3418	3417	-4.80	2.10	3.5	0.56	0.0918
	B	M4.0	3366	3356	-4.80	2.53	3.5	0.5	0.1147
GJ 2005 (LHS 1070)	A	M5.5	3160	3052	-4.43	6.88	3.5	2	0.1613
	B	M8.5	2450	2528	-4.43	15.85	0.3	~	5.9142
	C	M9.0	2400	2547	-4.43	15.04	0.3	~	6.1480

$T_{\text{eff}}^{(0)}$ is the temperature which corresponds to the spectral type of the star.

No accurate estimates of magnetic field were possible for stars with $v \sin i > 10$ km/s (marked with “~”)

Last column refer to the chi-square goodness of the fit (GOF) values.

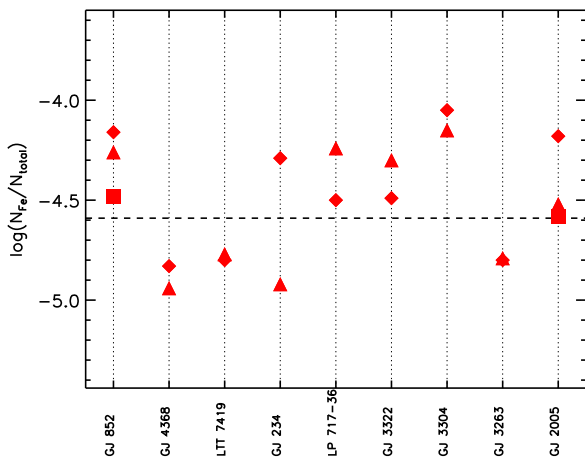


Figure 3. Derived iron abundance for *A* (diamonds), *B* (triangles), and *C* (squares) components of investigated dM systems. The reference solar abundance is shown by dashed horizontal line.

values for the atmospheric structure demonstrates the current difficulty to determine atmospheric parameters in the spectra of M-type dwarfs. To make progress on this part, independent information on metallicity or temperature are required, and improvements to our understanding of the damping coefficient are needed. Nevertheless, our investigation of different strategies (Cases 1–4) to fit the spectra shows that the uncertainty of atmospheric structure does not prevent us from determining the parameters we are most interested in this study: rotation velocity and magnetic field strength.

An important result of present spectroscopic investiga-

tion is that such key parameters as $v \sin i$ and $\langle B_s \rangle$ do not change much between different fitting cases that we considered. The only exception is Case 1 as explained in the previous section (fixing T_{eff} , $\alpha(\text{Fe})$, and $f(\gamma_{\text{Waals}})$ always provided an unreasonable fit). Thus, even if there are systematic uncertainties in estimated T_{eff} , $\alpha(\text{Fe})$, and/or $f(\gamma_{\text{Waals}})$, this does not significantly influence our results on $v \sin i$ and $\langle B_s \rangle$ so that our conclusions remain stable even if based on imperfect atmospheric descriptions.

With our measurements of rotation and magnetism we tried to answer two main questions:

- (i) How efficient is rotational braking in early- and late type components?
- (ii) How is this related to the intensity of the magnetic field?

A first result on spectral type dependent rotational braking in components of a multiple system was provided by Reiners et al. (2007) showing that the two late-M components in the triple system GJ 2005 rotate significantly faster than the early-M primary. We show the results of our rotation analysis in the left panel of Fig. 4. In all but one system, the earlier component rotates at a significantly lower rate than the later secondary. We interpret this as clear evidence for rotational braking being a strong function of spectral type, as expected from earlier work. The one exception are the *A* and *B* components of the triple system GJ 852, but their spectral types only differ by one subclass and we actually derive identical temperatures in our fits (even if we assume identical metallicity). In addition, components *A* and *B* in GJ 4368 and *B* and *C* in GJ 2005 appear to have rotational velocities identical within the uncertainties.

We also have three young systems in our sample: LP 717-36 and GJ 3304 are likely younger than 300 Myrs

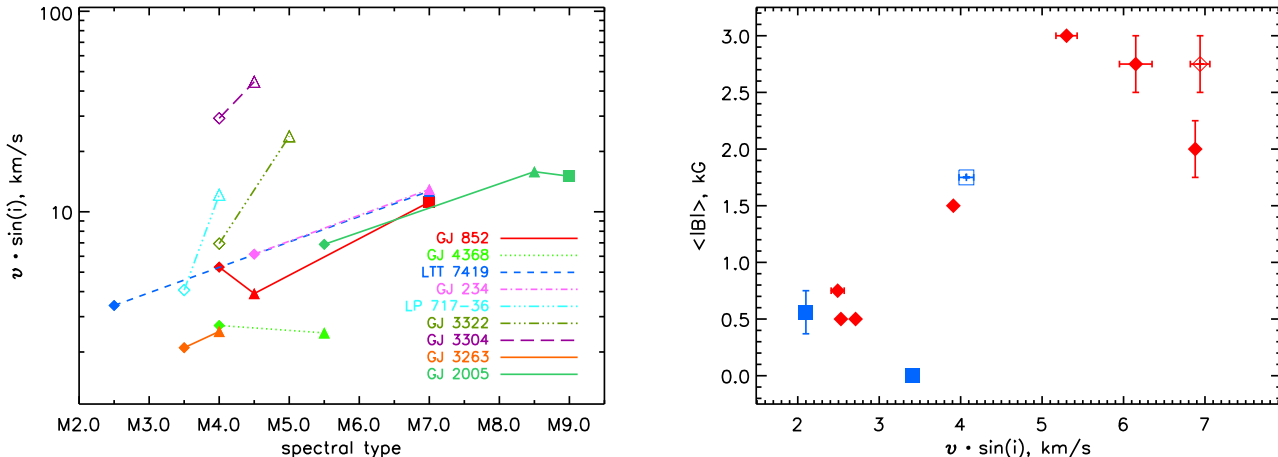


Figure 4. Graphical representation of main results from Table 4. **Left plot:** projected rotational velocity $v \sin i$ as a function of spectral type. Diamonds – primaries, triangles – secondaries, square – third components. **Right plot:** mean surface magnetic field intensity as a function of $v \sin i$ for stars with $v \sin i < 10$ km/s. Blue squares – stars of spectral type early than or equal to M4.0; red diamonds – stars of spectral type later than M4.0. Open symbols indicate young systems. Error bars correspond to the difference in $v \sin i$ and $\langle B_s \rangle$ between this case and Case 2.

(Shkolnik et al. 2009). GJ 3322 is a member of the β Pic moving group and thus probably even younger than 30 Myrs (Song et al. 2003). These three systems clearly stand out in Fig. 4 as the ones with the highest $v \sin i$ and showing the most extreme difference in rotation rates between their components. The latter is another indication that braking is less effective at later spectral types, even more so at young ages.

The reason for the difference in rotational braking is not entirely clear at this point. Stellar parameters like temperature, mass, and radius are changing rapidly among mid-M stars, and the change from partially to fully convective stars adds another complication to the interpretation because the influence of dynamo on the magnetic geometry is unknown. For the slowly rotating objects of our sample, we provide direct measurements of the average surface magnetic fields. In fast rotating stars with velocities $v \sin i > 10$ km/s, magnetic field estimates are highly uncertain because of strong line blending. Intensities of the mean surface magnetic fields $\langle B_s \rangle$ as a function of $v \sin i$ and spectral type are illustrated in the right panel of Fig. 4. We show only measurements in which Zeeman broadening was clearly seen and measurable, i.e. $v \sin i < 10$ km s $^{-1}$. There is a clear correlation between $\langle B_s \rangle$ and $v \sin i$; in our sample of M dwarfs, we find an increase in average magnetic field strength with $v \sin i$. This is an interesting result because we start to resolve the rising part of the unsaturated rotation-magnetic field relation (Reiners 2007), which was not possible before because of lower spectral resolving power.

The transition between partial to full convection is believed to occur around spectral type M3.5. There is only one system in our sample with a primary of spectral type earlier than M3.0 and six with spectral types of M4.0 and earlier. Nevertheless, an effect on magnetic field generation caused by a change in dynamo mode should not happen at a sharp threshold but rather take effect smoothly over a range of stellar masses. For example, all stars later than, say, M5.0 might be expected to have fields much higher than earlier

stars at the same rotation velocity, or the secondaries could have higher fields even if their rotation velocity does not significantly differ from the primary’s rotation rate. In our sample, we do not find evidence for any mechanism that requires explanation through the change in dynamo mode at the boundary to full convection. The differences in average magnetic field strength can be explained by the influence of rotation velocity alone. Our sample contains a few stars that are hot enough so that the influence of a tachocline could still be expected. Their distribution in velocity shows no difference to the late-M sample that probably generates magnetism without the presence of a tachocline.

6 SUMMARY

The results of this work can be summarized as follows:

- Among nine investigated spectroscopically resolved systems seven clearly have primaries that are rotating slower than less massive secondaries. In GJ 4368 both *A* and *B* were found to have comparable rotational velocities, as well as *B* and *C* in GJ 2005. Thus, we confirm the existence of spectral type dependent braking in low-mass stars, where the mid- and late type objects are braked less effectively compared to objects of earlier types.
- Three of the systems analysed here are younger than 300 Myrs. In all three of these system the secondary rotates considerably faster than in older systems with comparable spectral types, which is fully consistent with the assumption of differences in the braking efficiency with spectral type under a general Skumanich-type braking law.
- Strong surface magnetic fields were detected in primaries of five systems (GJ 852, GJ 234, LP 717-36, GJ 3322, GJ 2005), and also in secondary of the triple system GJ 852. No fields could be accurately detected in components with fast rotation.
- For slow and moderately rotating stars, there is a ten-

dency of the mean surface magnetic field to increase with the rotational velocity $v \sin i$.

- We find noticeable iron underabundance in such systems as GJ 4368, LTT 7419, and GJ 3263. However, taking into account other uncertainties (i.e. very fast rotation, γ_{Waals} , etc.) this should be considered with certain caution.

- Analysis of the spectra of inactive stars demonstrated that the van der Waals damping constant γ_{Waals} of FeH lines drops significantly in late-type objects compared to its classical value. This requires additional and more extensive investigation making use of extended sample of stars and spectra of better quality.

ACKNOWLEDGMENTS

This work was supported by the following grants: Deutsche Forschungsgemeinschaft (DFG) Research Grant RE1664/7-1 to DS and Deutsche Forschungsgemeinschaft under DFG RE 1664/4-1 and NSF grant AST07-08074 to AS. OK is a Royal Swedish Academy of Sciences Research Fellow supported by grants from the Knut and Alice Wallenberg Foundation and the Swedish Research Council. We also acknowledge the use of electronic databases (VALD, SIMBAD, NASA's ADS). This research has made use of the Molecular Zeeman Library (Leroy, 2004).

REFERENCES

- Afram, N., Berdyugina, S. V., Fluri, D. M., Solanki, S. K., Lagg, A. 2008, *A&A*, 482, 387
- Asensio Ramos, A., Trujillo Bueno, J. 2006, *ApJ*, 636, 548
- Asplund, M., Grevesse, N., & Sauval, A. J. 2005, in *ASP Conf. Ser. 336, Cosmic Abundances as Records of Stellar Evolution and Nucleosynthesis*, ed. Thomas G. Barnes III & Frank N. Bash, 25
- Barnes, S. A. 2007, *ApJ*, 669, 1167
- Bate, M. R., Bonnell, I. A., Clarke, C. J., Lubow, S. H., Ogilvie, G. I., Pringle, J. E., & Tout, C. A. 2000, *MNRAS*, 317, 773
- Bean, J. L., Sneden, C., Hauschildt, P. H., Johns-Krull, C. M., & Benedict, G. F. 2006, *ApJ*, 652, 1604
- Berdyugina, S. V., Solanki, S. K. 2002, *A&A*, 385, 701
- Berger, D. H., et al. 2006, *ApJ*, 644, 475
- Beuzit, J.-L., et al. 2004, *A&A*, 425, 997
- Buscombe, W., & Foster, B. E. 1995, Evanston, Illinois: Northwestern University, —c1995, edited by Buscombe, William —e(comp.); Foster, Bruce E. —e(ass.)
- Costa, E., Méndez, R. A., Jao, W.-C., Henry, T. J., Subasavage, J. P., Brown, M. A., Ianna, P. A., & Bartlett, J. 2005, *AJ*, 130, 337
- Daemgen, S., Siegler, N., Reid, I. N., & Close, L. M. 2007, *ApJ*, 654, 558
- Delfosse, X., Forveille, T., Beuzit, J.-L., Udry, S., Mayor, M., & Perrier, C. 1999, *A&A*, 344, 897
- Dulick, M., Bauschlicher, Jr., C. W., Burrows, A., Sharp, C. M., Ram, R. S., Bernath, P. 2003, *ApJ*, 594, 651
- Golimowski, D. A., Leggett, S. K., Marley, M. S., et al. 2004, *AJ*, 127, 3516
- Gray D.F. 1992, *The Observation and Analysis of Stellar Photospheres*, Cambridge University Press
- Gustafsson, B., Edvardsson, B., Eriksson, K., Jørgensen, U. G., Nordlund, Å., Plez, B. 2008, *A&A*, 486, 951
- Harrison, J. J., Brown, J. M. 2008, *ApJ*, 686, 1426
- Hawley, S. L., Gizis, J. E., & Reid, N. I. 1997, *AJ*, 113, 1458
- Herzberg, G. 1950 *Molecular Spectra and Molecular Structure. I. Spectra of Diatomic Molecules*, D. van Nostrand, Florida
- Jao, W.-C., Henry, T. J., Subasavage, J. P., Bean, J. L., Costa, E., Ianna, P. A., & Méndez, R. A. 2003, *AJ*, 125, 332
- Kawaler, S. D. 1988, *ApJ*, 333, 236
- Kenyon, S. J., Hartmann, L. 1995, *ApJS*, 101, 117
- Kirkpatrick, J. D., Henry, T. J., & McCarthy, D. W., Jr. 1991, *ApJS*, 77, 417
- Kochukhov, O. 2007, in *Physics of Magnetic Stars*, eds. D.O. Kudryavtsev and I.I. Romanyuk, Nizhnij Arkhyz., p.109
- Leinert, C., Allard, F., Richichi, A., & Hauschildt, P. H. 2000, *A&A*, 353, 691
- Lépine, S., Thorstensen, J. R., Shara, M. M., & Rich, R. M. 2009, *AJ*, 137, 4109
- Leroy, B. 2004, *Molecular Zeeman Library Reference Manual* (available on-line at <http://bass2000.obspm.fr/mzl/download/mzl-ref.pdf>)
- Mestel 1984, in *Third Cambridge Workshop on Cool Stars, Stellar Systems, and the Sun*, ed. S. L. Baliunas, & L. Hartmann (New York: Springer), 49
- Mohanty, S., & Basri, G. 2003, *ApJ*, 583, 451
- Monin, J.-L., Ménard, F., & Peretto, N. 2006, *A&A*, 446, 201
- Piskunov, N. 1999, *Astrophysics and Space Science Library*, 243, 515
- Reid, I. N., et al. 2004, *AJ*, 128, 463
- Reiners, A., 2007, *A&A*, 469, 259
- Reiners, A., & Basri, G. 2010, *ApJ*, 710, 924
- Reiners, A. & Basri, G. 2008, *ApJ*, 684, 1390
- Reiners, A. & Basri, G. 2007, *ApJ*, 656, 1121
- Reiners, A., Seifahrt, A., Käufl, H. U., Siebenmorgen, R., Smette, A. 2007, *A&A*, 471, L5
- Riaz, B., Gizis, J. E., & Harvin, J. 2006, *AJ*, 132, 866
- Ségransan, D., Kervella, P., Forveille, T., & Queloz, D. 2003, *A&A*, 397, L5
- Seifahrt, A., Röhl, T., Neuhäuser, R., et al., 2008, *A&A*, 484, 429
- Shkolnik, E., Liu, M. C., & Reid, I. N. 2009, *ApJ*, 699, 649
- Shulyak, D., Reiners, A., Wende, S., Kochukhov, O., Piskunov, N., Seifahrt, A. 2010, *A&A*, 523, A37
- Sills, A., Pinsonneault, M. H., & Terndrup, D. M. 2000, *ApJ*, 534, 335
- Skumanich, A. 1972, *ApJ*, 171, 565
- Song, I., Zuckerman, B., & Bessell, M. S. 2003, *ApJ*, 599, 342
- Sterzik, M. F., & Tokovinin, A. A. 2002, *A&A*, 384, 1030
- Wende, S., Reiners, A., Seifahrt, A., Bernath, P. F. 2010, *A&A*, 523, A58